Title	Synthesized effective atomic numbers for commercially available dual-energy CT
Author(s)	Kawahara, Daisuke; Ozawa, Shuichi; Yokomachi, Kazushi; Fujioka, Chikako; Kimura, Tomoki; Awai, Kazuo; Nagata, Yasushi
Citation	Reports of Practical Oncology and Radiotherapy , 25 (4) : 692 - 697
Issue Date	2020
DOI	10.1016/j.rpor.2020.02.007
Self DOI	
URL	https://ir.lib.hiroshima-u.ac.jp/00050442
Right	© 2020. This manuscript version is made available under the CC-BY-NC-ND 4.0 license http://creativecommons.org/licenses/by-nc-nd/4.0/ This is not the published version. Please cite only the published version. この論文は出版社版ではありません。引用の際には出版社版をご確認、ご利用ください。
Relation	

~~Technical note:~~ Synthesized effective atomic numbers for commercially available dual-energy CT

Daisuke Kawahara.[1], Shuichi Ozawa, Ph.D.[1,2], Kazushi Yokomachi[3], Chikako Fujioka[3], Tomoki Kimura, Ph.D.[1], Kazuo Awai, Ph.D.[4], Yasushi Nagata[1,2]

1) Department of Radiation Oncology, Institute of Biomedical & Health Sciences, Hiroshima University

2) Hiroshima High-Precision Radiotherapy Cancer Center

3) Radiation Therapy Section, Division of Clinical Support, Hiroshima University Hospital

4) Department of Radiation Oncology, Graduate School of Medicine, Hiroshima University,

Corresponding author: Daisuke Kawahara.

Department of Radiation Oncology, Institute of Biomedical & Health Sciences, Hiroshima University

Tel: +81-82-257-5561

Fax: +81-82-257-5561

E-mail: daika99@hiroshima-u.ac.jp

Keyword: effective atomic numbers, dual-energy CT, monochromatic CT number, beam-hardening

Conflict of Interest Notification: none

ABSTRACT

Purpose: The objective of this study was to assess synthesized effective atomic number (Z_{eff}) values with a new developed tissue characteristic phantom and contrast material of varying iodine concentrations using single-source fast kilovoltage switching dual-energy CT (DECT) scanner.

Methods: A newly developed multi energy tissue characterisation CT phantom and an acrylic phantom with various iodine concentrations of were scanned using single-source fast kilovoltage switching DECT (GE-DECT) scanner. The difference between the measured and theoretical values of Z_{eff} were evaluated. Additionally, the difference and coefficient of variation (CV) values of the theoretical and measured values were compared with values obtained with the Canon-DECT scanner that was analysed in our previous study.

Results: The average Z_{eff} difference in the Multi-energy phantom was within 4.5%. The average difference of the theoretical and measured Z_{eff} values for the acrylic phantom with variation of iodine concentration was within 3.3%. Compared to the results for the single-source Canon-DECT scanner used in our previous study, the average difference and CV of the theoretical and measured Z_{eff} values obtained with the GE-DECT scanner were markedly smaller.

Conclusions: The accuracy of the synthesized Z_{eff} values with GE-DECT had a good agreement with the theoretical Z_{eff} values for the Multi-Energy phantom. The GE-DECT could reduce the noise and the accuracy of the Z_{eff} values than that with Canon-DECT for the varying iodine concentrations of contrast medium.

Advances in knowledge: The accuracy and precision of the Z_{eff} values of the contrast medium with the GE-DECT could be sufficient with human equivalent materials.

Introduction

Dual-energy computed tomography (DECT) enables direct calculation of the effective atomic number (Z_{eff}), the monochromatic energy CT number, and electron density on pixel by pixel basis [1,2]. The beam hardening artefact can be reduced by DECT and DECT provide more quantitatively accurate attenuation measurements [3-5]. Additionally, DECT can estimate iodine content in tissues by using the iodine map [6,7]. In clinic, DECT has been applied to bone removal, and the automatic characterization of stone compositions [8-10].

Various commercial DECT scanners are available that can acquire CT datasets at two different energies: a single-source dual-energy scanner with fast kilovoltage switching; a dual-source, dual-energy scanner; a single-source CT scanner that switches kilovoltages between gantry rotation; and a single-source, dual-energy scanner with two detector layers. In the current study, the dual-energy scanner with fast kilovoltage switching is used. The advantages of DECT with fast kilovoltage switching is temporal registration between two-different energy datasets, that are acquired simultaneously.

Mitchell et al. evaluated the accuracy of the Z_{eff} values that were calculated with fast kilovoltage switching with a single detector layer with a GE Discovery CT750 DECT scanner (GE Healthcare, Princeton, NJ, USA) [11]. They investigated the accuracies of the synthesized effective atomic number and monochromatic images maps. Recently, a new DECT system, Revolution HD CT(GE-DECT) scanner (GE Healthcare, Milwaukee, WI), has been developed. This scanner is expected to improve the accuracy of the Z_{eff} values compared to Discovery CT750 HD scanner (GE Healthcare, Milwaukee, WI). It is able to be expected to improve the accuracy of the Z_{eff} values using the Revolution HD CT.

DECT has the advantage that it can create the iodine maps image [12]. The lesion target and normal tissue delineation, extraction of the blood vasculature could be achieved by quantification of the iodine concentration in cancers. An iodine distribution map is a promising tool for predicting the tumor response after treatment for cancers. Lee et al. showed that there is a possibility to distinguish between different cancers by quantifying iodine concentration [13]. But, before the iodine distribution map can be used clinically, it is necessary to understand the accuracy of iodine quantitation with DECT. Our previous study investigated the accuracy of the estimated Z_{eff} values for varying iodine concentrations of contrast medium (CM) compared with the theoretical Z_{eff} values using a single-source CT that switches voltages between gantry rotations, as implemented in Canon Aquilion ONE™ DECT scanner (Canon-DECT) (Canon Medical Systems Corporation, Ōtawara-shi, Japan). In the current study we found that the average difference between the theoretical and estimated Z_{eff} values for the CM was within 11.2% [14].

The aim of the current study was to assess a new developed phantom with inserts of tissue material that replicates expected Hounsfield unit (HU) dependencies from low energy to high energy using the GE-DECT. Moreover, the accuracy of the synthesized Z_{eff} values with contrast material of varying iodine concentrations using the GE-DECT were evaluated, and the comparison of the Z_{eff} values of the GE-DECT and the Canon-DECT was performed.

Methods and Materials

A) Data acquisition:

The current study used following different DECT scanners: a) the Revolution DECT scanner (GE Healthcare, Princeton, NJ, USA) which will be referred to as GE-DECT, and b) the Canon Aquilion ONE™ (Canon Medical Systems Corporation, Ōtawara-shi, Japan) which will be referred to as Canon-DECT. The scan data was obtained from previous study [13)]. The GE-DECT scanned at 80 and 140 kV tube voltages and exposures of 560 mA were used. The other scanning parameters were field of view (FOV) of 360 mm, slice thickness (ST) of 0.5 mm, and a rotation time (RT) of 1.0 s. The 72 middle slices of a total of 80 slices was analysed. The Canon-DECT was scanned at tube voltages of 135 and 80 kV using the volume scanning method. The exposures were 800 and 200 mA, and the time taken to switch the tube voltage between 135 and 80 kV was 0.4 s. The other parameters were FOV of 400 mm, ST of 0.5 mm, and a RT of 1.0 s. The Z_{eff} was reconstructed from the scanned DECT image. Also, the 70 keV monoenergetic CT image was reconstructed from the scanned DECT image to evaluate the accuracy of the iodine concentration.

B) Phantom:

Two phantom were scanned: 1) A Multi-Energy phantoms with inserts of varying iodine and calcium concentrations (Sun Nuclear, Middleton, WI, USA) (Figure 1a), and 2) an in-house developed acrylic phantom with inserts syringes filled with different iodine concentrations (Figure 1b). The size of the acrylic phantom is 32 cm Ø and 6 cm height. The syringes filled with CM (Omnipaque 300, GE Healthcare, Prnceton, NJ, USA) diluted water to predetermined iodine concentrations of 0, 1, 2, 3, 4, 5, 6, 7, 8, 9, 10, 20, 40, 60, 90, and 130 mg iodine per ml. Here, the syringes filled with the CM used in the current study were created in our previous study [13]. The syringe was not emptied and refilled between the current and previous studies.

Multi-Energy CT phantom can improve material decomposition in clinical, such as distinguishing calcification from iodinated contrast and blood from calcification [15]. However, the maximum concentration of the CM in the Multi-Energy phantom is 15 mg/ml. Jang et al. reported that Lipiodol, which is used in trans-arterial chemoembolization (TACE), had a larger CT number, and its value was over 2000 HU at maximum [16]. Our previous study showed the correlation of the CT number and the concentration of the CM. A high concentration of the CM at over 20 mg/ml has been used for TACE. Thus, the current study evaluates the Z_{eff} values for high concentrations of the CM at over 20 mg/ml with the in-house developed CM phantom.

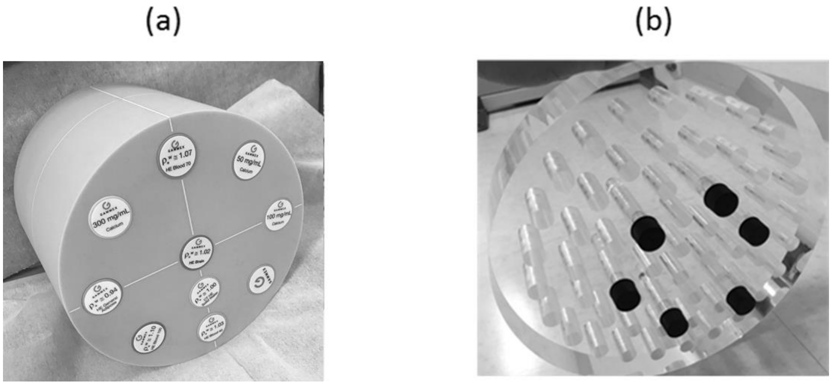

Figure 1 (a) Multi-Energy phantom, (b) Acrylic phantom with variation of iodine concentration of CM.

C) Theoretical Z_{eff} value:

The theoretical Z_{eff} values for the Multi-energy phantom and acrylic phantom with CM were calculated using Mayneord's equation [17]:

$$Z_{\text{eff}} = \sqrt[2.94]{\sum_{i=1}^{n} a_i Z_i^{2.94}} \quad (1)$$

where Z_i is the atomic number and a_i is the fractional of the electrons in the *i*-th element in the mixture to the total number of electrons. The material composition information is used rereleased by the manufacturer.

D) Measured Z_{eff} value:

The Z_{eff} image reconstructed by GE and Canon DECT scanners was analyzed using the ImageJ (National Institutes of Health, Bethesda, MD, USA). The effect of the beam hardening was evaluated by measuring the centre and peripheral region as shown in Figure 2(a). The syringe was filled with the water only. A circular region of interest (ROI) for each image was drawn within 0.8 cm area in the syringe. The mean (M) and standard deviation (SD) of the Z_{eff} values within a circular ROIs for each slice were measured. The average of the M and SD for 72 slices were evaluated. For the evaluation of the CM, the M, SD, and coefficient of variation (CV) of the Z_{eff} values in the syringes were evaluated. The CV is the ratio of the standard deviation to the average Z_{eff} values in the different pixels of the ROI, as follows.

$$CV = SD/\mathrm{M} \quad (2)$$

The average of M, SD, and CV of the Z_{eff} values for 72 slices were evaluated for the syringe with the CM. The ROI for each image were drawn within 0.8 cm area in the syringe. At low concentration of the CM, the mean Z_{eff} value is smaller, thus the effect of the SD might be larger, relatively. Thus, the CV was used to evaluate the variation in the images at low and high concentrations of the CM. The proportionality of contrast enhancement to iodine concentration is near constant within 15 mg/ml [18)]. Thus, the current study assumed that the correlation of the CT number and iodine concentration was fitted to a linear function. The concentration was calculated from the CT number with a linear function, which was compared with the iodine concentration which we defined. Thus, the mean and SD of the CT numbers at 70 keV image reconstructed from the GE-DECT in the syringe with the iodine concentration within 10 mg/ml were evaluated. For the Multi-energy phantom, the method of the measurement was the same with the CM. A circular ROI for each image was drawn within 0.8 cm area in the material inserts. The M and SD of the Z_{eff} values within a circular ROIs for each slice were measured. The average of the M and SD for 72 slices were evaluated.

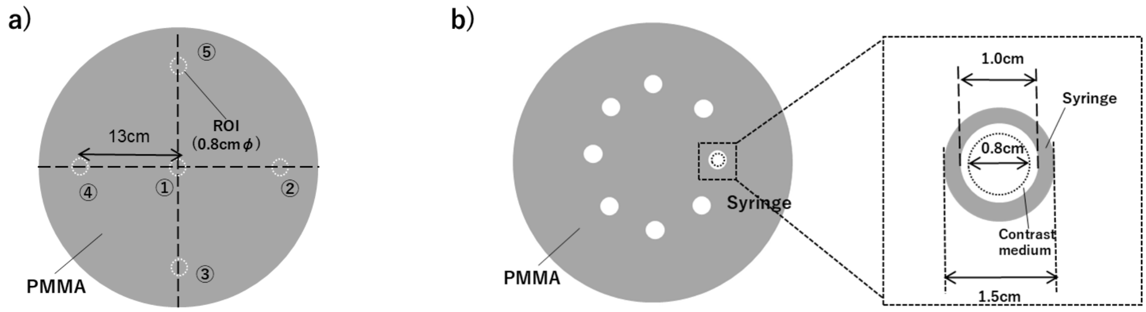

Figure 2. (a) Method of measurement with the acrylic phantom by the beam hardening effect. The distance of the center of the ROI and peripheral of the ROI was 13 cm. The mean and SD were measured by creating a circular ROI with 0.8 cm. (b) Method of measurement with the acrylic phantom that inserted the syringes filled with CM that the diameter is 1cm in a syringe that the diameter was 1.5 cm. The mean and SD were measured by creating a circular ROI with 0.8 cm diameter in the syringe.

E) Evaluation:

In the current study, the following items were investigated. i) The accuracy of the Z_{eff} values in the Multi-Energy phantom. ii) The accuracy of the Z_{eff} values for the CM phantom. The measured Z_{eff} values were compared with theoretical values and the relative average differences were calculated. The accuracy of the Z_{eff} values with the GE-DECT was compared with the Canon-DECT. iii) The difference of the CV values between the GE-DECT and the Canon-DECT.

Results

A) Accuracy of the iodine concentration:

Figure 3 shows the correlation of the iodine concentration and the CT number at 70 keV. The current study assumed that the correlation of the CT number and iodine concentration was fitted to a linear function. The proportionality of contrast enhancement to iodine concentration is near constant. The maximum difference of the estimated iodine concentration and the concentration which we defined was 3.5% at the iodine concentration of 0–10 mg/ml.

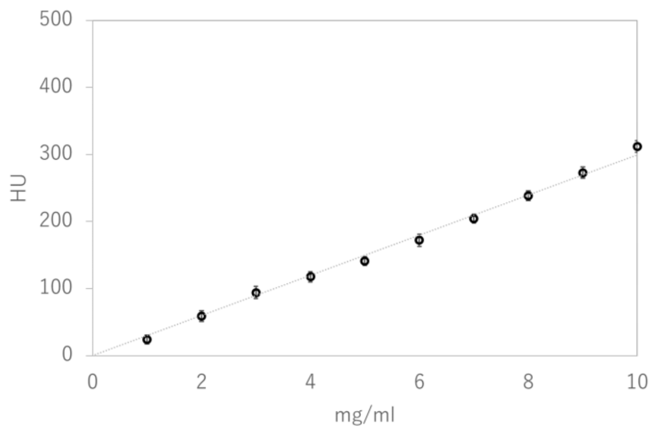

Figure 3 The average of M and SD of the Z_{eff} values at iodine concentrations of 0–10 mg/ml for 72 slices. The fitting was performed with linear function.

B) Reproducibility of the measured Z_{eff} values and effect of the beam hardening:

Figure 4(a) shows the Z_{eff} values in the centre and peripheral region. The maximum difference of the Z_{eff} values in the centre region and peripheral region was 0.01. The beam hardening effect is significantly smaller than the SD of the Z_{eff} values. Figure 4(b) shows the reproducibility of the measurement Z_{eff} value. The difference of the Z_{eff} values for three scans was within the SD of the Z_{eff} values.

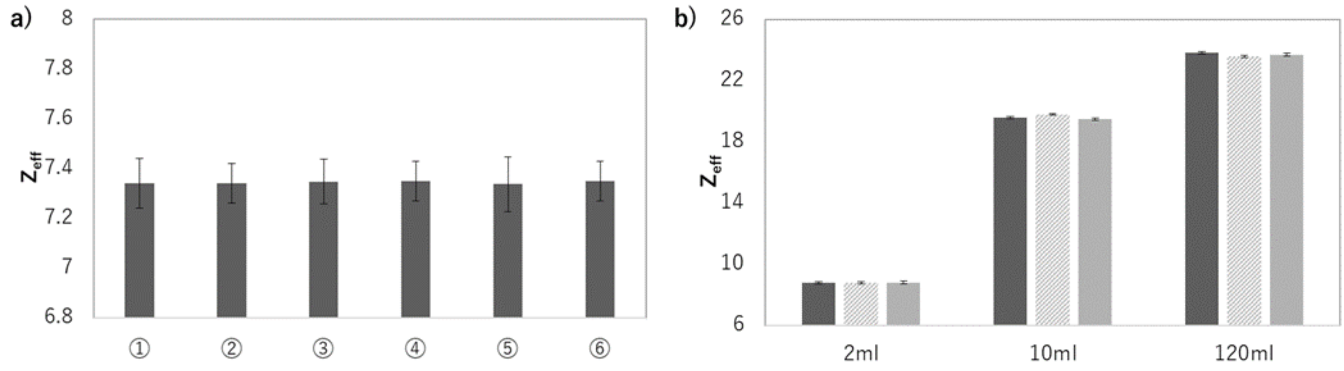

Figure 4 (a) The average of the M of the measurement Z_{eff} values in the center and peripheral region for 72 slices. The error bar represents the average of the SD of the measurement Z_{eff} values for 72 slices. (b) Reproducibility of the measurement Z_{eff} value for three scans. The error bar represents the SD of the measurement Z_{eff} value for three scans.

Figure 5 (a) represents the theoretical Z_{eff} values and the average M and SD of the measured Z_{eff} values, and Figure 5 (b) represents the deviation between the theoretical Z_{eff} values and the measured Z_{eff} values in the Multi-Energy phantom. As shown in Figure 5 (b), the difference of the Z_{eff} values for all material inserts were within 5.1%. The average and SD of the difference of theoretical and measurement Z_{eff} values for all material inserts were 2.5% and 1.4%. Figure 6 (a) represents the theoretical Z_{eff} values and the average M and SD of the measured Z_{eff} values, Figure 6 (b) represents the deviation between the theoretical Z_{eff} values and the measured Z_{eff} values in the acrylic phantom. The Z_{eff} values were larger at higher concentration of the CM. The maximum standard deviation of the CM was within 0.1. As shown in Figure 6 (b), the maximum difference was within 0.6%. At the low concentration of the CM within 10 mg/ml, the deviation between the theoretical Z_{eff} values and the average measured Z_{eff} values were scattered. Figure 7 represents the difference of the Z_{eff} values in the CM scanned by the GE-DECT that was measured in the current study and the Canon-DECT that was found in our previous study. The average difference of the Z_{eff} values was within 3.3% at the range of 0-130 mg/ml with the GE-DECT. In comparison, the average difference of the theoretical and measured Z_{eff} values with the Canon-DECT was within 7.2% at less than 20 mg/ml, and the maximum difference was 11.2% at 130 mg/ml. The difference of the theoretical and measured Z_{eff} values was smaller with GE-DECT. Figure 8 shows the CV values with the GE-DECT and the Canon-DECT. The difference of the CV values due to the concentration of the CM was small with the Canon-DECT, but it was larger in low concentration at less than 20 mg/ml with the Canon-DECT. At the low concentration of the CM within 10 mg/ml, the CV values were scattered for both oof GE-DECT and Canon-DECT. The CV values with the GE-DECT was significantly smaller than that with the Canon-DECT at all iodine concentration of the CM.

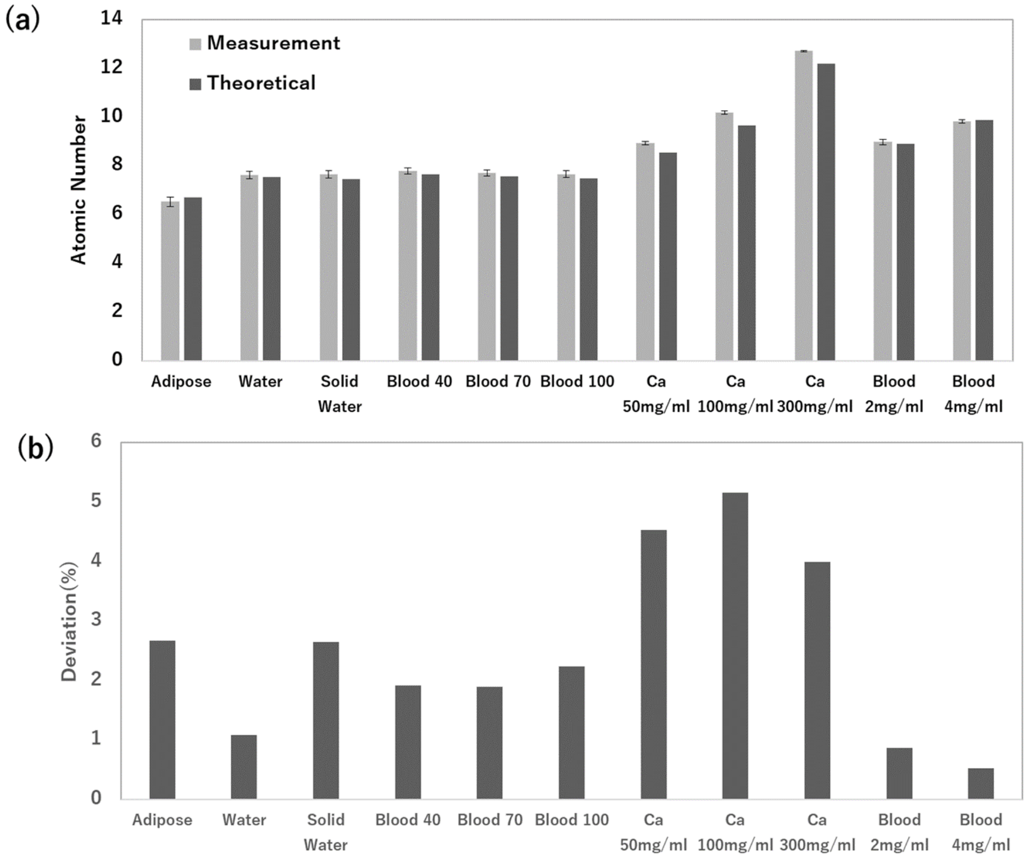

Figure 5 (a) The theoretical Z_{eff} values and the average measured Z_{eff} values. Error bars represent standard deviation of the average values. (b) The deviation between the theoretical Z_{eff} values and the average measured Z_{eff} values in the Multi-Energy phantom.

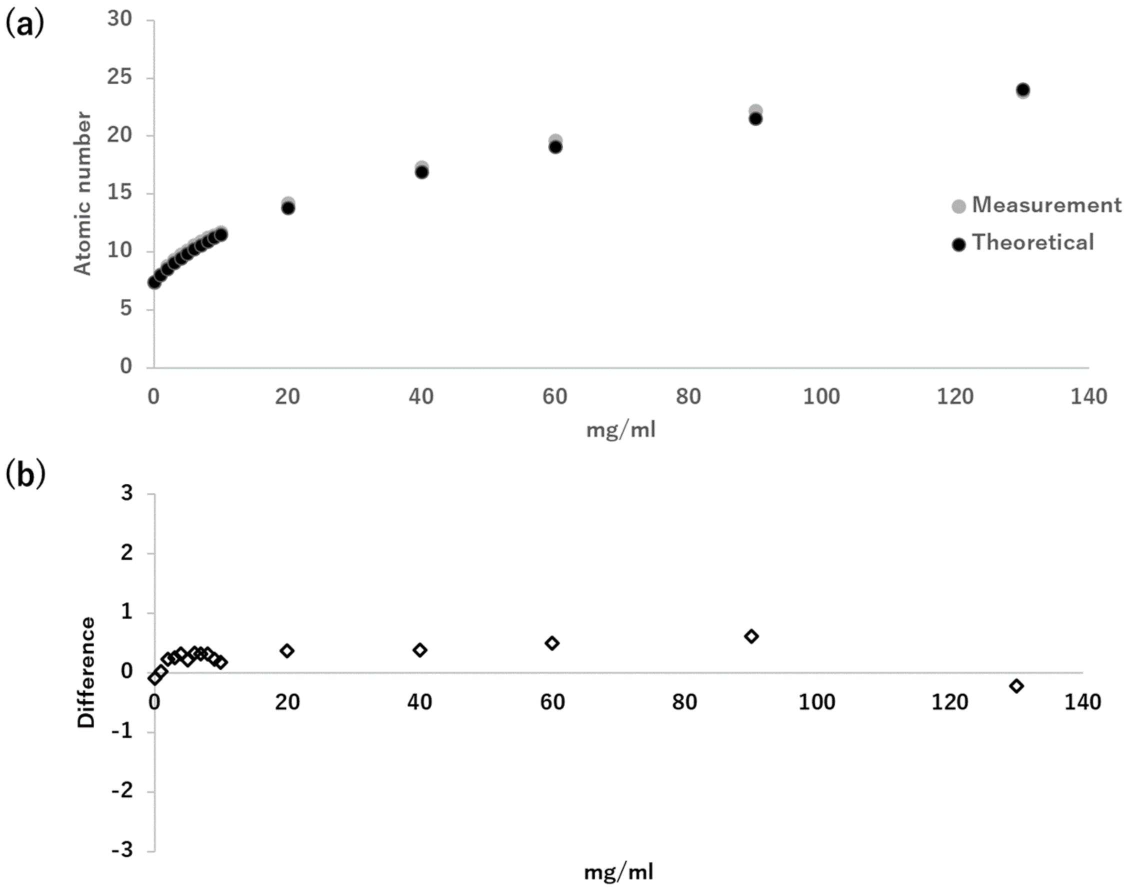

Figure 6 (a) The theoretical Z_{eff} values and the average measured Z_{eff} values. (b) The deviation between the theoretical Z_{eff} values and the average measured Z_{eff} values in the acrylic phantom with variation of iodine concentration of CM.

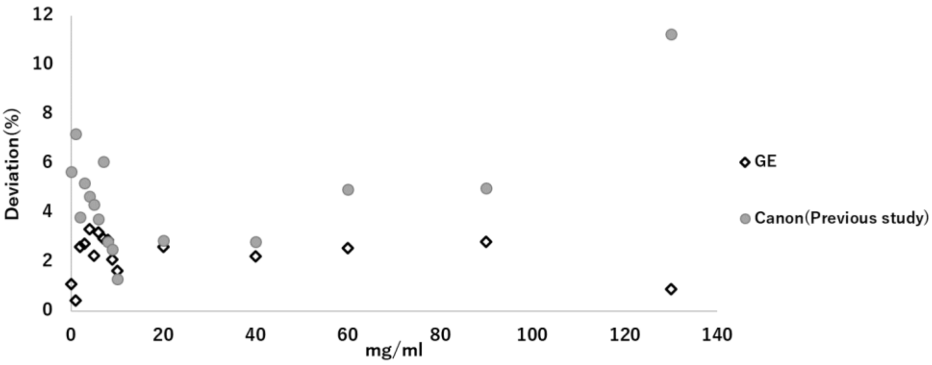

Figure 7 The difference of the theoretical and measured Z_{eff} values with the GE-DECT and the Canon-DECT in the acrylic phantom with variation of iodine concentration of CM.

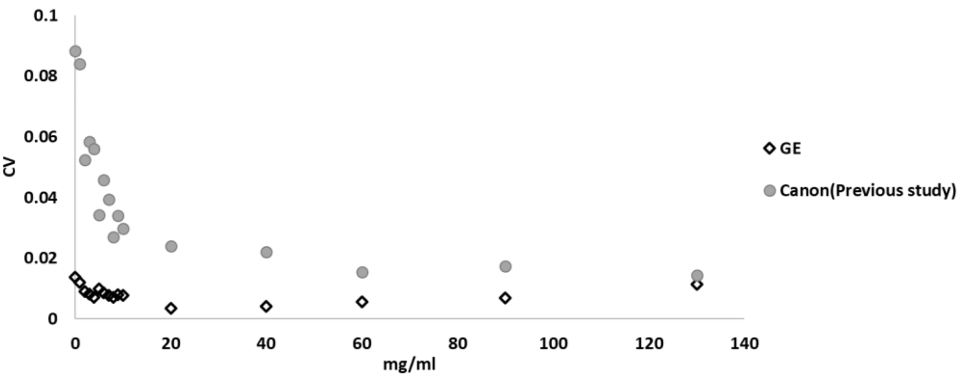

Figure 8 The difference of the CV of the Z_{eff} values with the GE-DECT and the Canon-DECT in the acrylic phantom with variation of iodine concentration of CM.

Discussion

This study evaluated the accuracy of Z_{eff} values in tissue equivalent materials and the CM. The past study reported the accuracy of the Z_{eff} values with various DECT scanner types and various tissue-equivalent phantoms. The past study reported the accuracy of the Z_{eff} values with various DECT scanner types and various tissue equivalent phantoms. Mitchell, et al. investigated the accuracy of the Z_{eff} values estimated from DECT scans acquired with a Discovery CT750 DECT scanner; they found the Zeff values of the Catphan phantom and tissue characterization were within 15% [10]. In the current study, Revolution HD CT was used. The accuracy of the Z_{eff} values in tissue equivalent phantom was within 4.5%. The average and SD of the difference of Z_{eff} values in tissue equivalent phantom was within 2.5% and 1.4%, respectively. The Revolution CT has enabled increasing 20% energy separation between the high and low energies by improving generator hardware enabling faster kV to rise and fall times by comparing with Discovery CT750 HD [19]. Thus, the beam hardening artefact and the noise could be reduced [20]. Material discrimination could be accurate by increasing spectral separation [16]. This contributed to the improved accuracy of the Z_{eff} values using the Revolution HD CT. Moreover, our previous study evaluated Z_{eff} values in raw-data based reconstruction image with the Canon-DECT implicated by Canon for the tissue equivalent phantom [13]. The accuracy except of the lung inserts were within 8.4%. The Canon-DECT was scanned with 135 kV and 80 kV, thus the higher kV energy was lower than the GE-DECT implicated by GE Healthcare. This could potentially result in an increased spectral separation that contribute to the reduced noise and better material discrimination.

For the acrylic phantom with the syringe filled with the CM, the beam hardening artefact was smaller and the reproducibility was significantly smaller than the SD of the Z_{eff} values in the ROI. Thus, the reliability of the measurement Z_{eff} values was sufficient. The accuracy of the Z_{eff} values was within 3.3% at the range of 0-130 mg/ml in the CM with the GE-DECT. It could be also the higher beam was used the DECT implicated by GE Healthcare, which could reduce the beam hardening artefact with the high concentration of the CM.

At the low concentration of the CM within 10 mg/ml, the CV and the deviation between the theoretical Z_{eff} values and the average measured Z_{eff} values were scattered, as shown in Figure 6(b) and Figure 8. At the low concentration of the CM, the mean value of the Zeff is close to 0. Thus, the SD in the images significantly affects the deviation and CV. Moreover, the

CV is larger at the low concentration of the CM even if the SD is the same value between low and high concentrations of the CM.

Although the accuracy of the Z_{eff} values was within 7.2% at less than 20 mg/ml in the CM, the beam hardening artefact was affected at over 20 mg/ml and the maximum difference was 11.2% at 130 mg/ml with the Canon-DECT. For the GE-DECT, the accuracy of the Z_{eff} values was within 3.3% at the range of 0-130 mg/ml in the CM. Moreover, the CV with the GE-DECT was significantly smaller than the Canon-DECT. It depends on that the SD was smaller for the GE-DECT. The image reconstruction method and imaging filter, and the deviation of the high and low-kV energy were affected these differences. In clinical of radiation diagnosis, the accuracy and precision of the Z_{eff} values within 15 mg/ml are needed. From above, the GE-DECT could be useful for the material decomposition.

In our previous study, the CM extraction method was developed, but it used only electron density and CT data [20]. However, they did not show the accuracy of the electron density. The current study revealed that the accuracy and the precision of the Z_{eff} values were sufficient for the material decomposition. It is possible to contribute to improving the estimation accuracy of the CM distribution by adding the Z_{eff} values. The accuracy and precision were different between the DECT scanner types, thus the data such as electron density and Z_{eff} obtained from DECT should be evaluated before using for the material decomposition in clinical.

Conclusion

The accuracy of the synthesized Z_{eff} values with dual-source DECT was in good agreement with theoretical values for the Multi-Energy phantom. The GE-DECT could reduce the noise and improve the accuracy of the Z_{eff} values compared to a Canon-DECT for the varying iodine concentrations of CM.

References

1. Meier A, Wurnig M, et al. Advanced virtual monoenergetic images: improving the contrast of dual-energy CT pulmonary angiography. Clin Radiol. 2015 Nov;70(11):1244-51
2. Yang M, Virshup G, Clayton J, Zhu XR, Mohan R, Dong L (2010) Theoretical variance analysis of single- and dual-energy computed tomography methods for calculating proton stopping power ratios of biological tissues. Phys Med Biol 55:1343–1362
3. Wohlfahrt P, Möhler C, Hietschold V, et al. Clinical Implementation of Dual-energy CT for Proton Treatment Planning on Pseudo-monoenergetic CT scans. Int J Radiat Oncol Biol Phys. 2017 Feb 1;97(2):427-434.
4. Marin, D., Boll, D.T., Mileto, A. and Nelson, R.C. 2014. State of the art: dual-energy CT of the abdomen. Radiology. 271: 327–342.
5. Yu L, Leng S, McCollough CH. Dual-energy CT-based monochromatic imaging. AJR Am J Roentgenol. 2012 Nov;199(5 Suppl):S9-S15.Kaemmerer N, Brand M, et al. Dual-Energy Computed Tomography Angiography of the Head and Neck With Single-Source Computed Tomography: A New Technical (Split Filter) Approach for Bone Removal. Invest Radiol. 2016 Oct;51(10):618-23
6. Zhang LJ, Wu S, Wang M, et al. Quantitative dual energy CT measurements in rabbit VX2 liver tumors: Comparison to perfusion CT measurements and histopathological findings. Eur J Radiol 2012; 81: 1766–75.
7. Stiller W, Skornitzke S, Fritz F, et al. Correlation of quantitative dual-energy computed tomography iodine maps and abdominal computed tomography perfusion measurements: are single-acquisition dual-energy computed tomography iodine maps more than a reduced-dose surrogate of conventional computed tomography perfusion? Invest Radiol 2015; 50: 703–8.

8. Primak AN, Fletcher JG, et al. Noninvasive differentiation of uric acid versus nonuric acid kidney stones using dual-energy CT. Acad Radiol 2007;14:1441–1447

9. Nicolaou S, Yong-Hing CJ, et al. Dual-energy CT as a potential new diagnostic tool in the management of gout in the acute setting. AJR 2010; 194:1072–1078

10. Mitchell M. Goodsitt, et al. Accuracies of the synthesized monochromatic CT numbers and effective atomic numbers obtained with a rapid kVp switching dual energy CT scanner. Med Phys 2011;38(4):2222–32

11. Kang M-J, Park CM, et al. Dual-energy CT: clinical applications in various pulmonary diseases. Radiographics. 2010;30(3):685–98

12. Lee SH, Hur J, Kim YJ, Lee HJ, et al. Additional value of dual-energy CT to differentiate between benign and malignant mediastinal tumors: an initial experience. Eur J Radiol. 2013;82(11):2043–49

13. Kawahara D, Ozawa S, et al. Accuracy of the raw-data-based effective atomic numbers and monochromatic CT numbers for contrast medium with a dual-energy CT technique. Br J Radiol. 2018 Feb;91(1082):20170524.

14. Nute JL, Jacobsen MC, et al. Dual-Energy Computed Tomography for the Characterization of Intracranial Hemorrhage and Calcification: A Systematic Approach in a Phantom System. Invest Radiol. 2017 Jan;52(1):30-41.

15. Ishikawa T, Abe S, et al. Cone-Beam Computed Tomography Correlates with Conventional Helical Computed Tomography in Evaluation of Lipiodol Accumulation in HCC after Chemoembolization. PLoS One. 2016 Jan 11;11(1): e0145546.

16. McCollough, et al. Dual- and Multi-Energy CT: Principles, Technical Approaches, and Clinical Applications, Radiology. 276(3): 637-653, (2015).

17. W. V. Mayneord. The significance of the roentgen. Acta of the International Union Against Cancer, 1937;2:271–282.

18. Bae KT. Intravenous contrast medium administration and scan timing at CT: considerations and approaches. Radiology. 2010 Jul;256(1):32-61.

19. Slavic et al, Technology White Paper, GSI Xtream on RevolutionTM CT, 2017.

20. Kawahara D, Ozawa S, et al. Automatic contrast medium extraction system using electron density data with dual-energy CT. Br J Radiol. 2018 Jul 9:20180396.

Figure legends

Figure 1 (a) Multi-Energy phantom, (b) Acrylic phantom with variation of iodine concentration of CM.

Figure 2. (a) Method of measurement with the acrylic phantom by the beam hardening effect. The distance of the center of the ROI and peripheral of the ROI was 13 cm. The mean and SD were measured by creating a circular ROI with 0.8 cm. (b) Method of measurement with the acrylic phantom that inserted the syringes filled with CM that the diameter is 1cm in a syringe that the diameter was 1.5 cm. The mean and SD were measured by creating a circular ROI with 0.8 cm diameter in the syringe.

Figure 3 The mean and SD for the Z_{eff} values at iodine concentrations of 0–10 mg/ml. The fitting was performed with linear function.

Figure 4 (a) The mean and SD of the Z_{eff} values in the center and peripheral region. (b) Reproducibility of the measurement Z_{eff} value for three scans. The error bar represents the SD of the measurement Z_{eff} value for three scans.

Figure 5 (a) The theoretical Z_{eff} values and the average measured Z_{eff} values. Error bars represent standard deviation of the average values. (b) The deviation between the theoretical Z_{eff} values and the average measured Z_{eff} values in the Multi-Energy phantom.

Figure 6 (a) The theoretical Z_{eff} values and the average measured Z_{eff} values. (b) The deviation between the theoretical Z_{eff} values and the average measured Z_{eff} values in the acrylic phantom with variation of iodine concentration of CM.

Figure 7 The difference of the theoretical and measured Z_{eff} values with the GE-DECT and the Canon-DECT in the acrylic phantom with variation of iodine concentration of CM.

Figure 8 The difference of the CV of the Z_{eff} values with the GE-DECT and the Canon-DECT in the acrylic phantom with variation of iodine concentration of CM.